Comparison of acquisition techniques for GNSS signal processing in geostationary orbit

Benjamin Chibout, Christophe Macabiau, Anne-Christine Escher, Lionel Ries, Jean-Luc Issler, Stéphane Corazza, Michel Bousquet

Comparison of Acquisition Techniques for GNSS Signal Processing in Geostationary Orbit

B. Chibout, C. Macabiau, A-C. Escher, *Ecole Nationale de l'Aviation Civile/Tesa*
L. Ries, J-L. Issler, *CNES*
S. Corrazza, *AlcatelAleniaSpace*
M. Bousquet, *Supaero*

BIOGRAPHY

Benjamin Chibout is a Ph.D. student in the field of GPS space application in the signal processing lab of the Ecole Nationale de l'Aviation Civile (ENAC) in Toulouse, France. He graduated in 2004 as an electronics engineer from the ENAC, and received the same year his Master research degree in signal processing.

Christophe Macabiau graduated as an electronics engineer in 1992 from ENAC in Toulouse, France. Since 1994, he has been working on the application of satellite navigation techniques to civil aviation. He received his Ph.D. in 1997 and has been in charge of the signal processing lab of the ENAC since 2000.

Anne-Christine ESCHER graduated as an electronics engineer in 1999 from the ENAC in Toulouse, France. Since 2002, she has been working as an associated researcher in the signal processing lab of the ENAC. She received her Ph.D. in 2003.

Lionel Ries is a navigation engineer in the "Transmission Techniques and Signal Processing Department", at CNES since June 2000. He is responsible of research activities on GNSS2 signals, including BOC modulations and modernised GPS signals (L2C & L5). He graduated from the Ecole Polytechnique de Bruxelles, at Brussels Free University (Belgium) and then specialized in space telecommunications systems at Supaero (ENSAE), in Toulouse (France).

Jean-Luc Issler is head of the Transmission Techniques and signal processing department of CNES, whose main tasks are signal processing, air interfaces and equipments in Radionavigation, TT&C, propagation and spectrum survey. He is involved in the development of several spaceborne receivers in Europe, as well as in studies on the European RadioNavigation projects, like GALILEO and the Pseudolite Network. With DRAST and DGA, he represents France in the GALILEO Signal Task Force of the European Commission. With Lionel Ries and Laurent Lestarquit , he received the astronautic prize 2004 of the French Aeronautical and Astronautical Association (AAAF) for his work on Galileo signal definition.

Stéphane Corazza is a research and development engineer in Alcatel Alenia Space company. He has experience in GPS and Galileo receivers design, digital signal processing suited to radiocommunications and satellite navigation, ASIC and FPGA development for satellite digital payloads. He has received engineering degree in Electronics and Telecommunication in the National Institute of Applied Sciences (INSA - Lyon, France, 1994).

Michel Bousquet is a Professor at SUPAERO (French Aerospace Engineering Institute of Higher Education), in charge of graduate and post-graduate programs in aerospace electronics and communications. He has over twenty five years of teaching and research experience, related to many aspects of satellite systems (modulation and coding, access techniques, onboard processing, system studies...). He has authored or co-authored many papers in the areas of digital communications and satellite communications and navigation systems, and textbooks, such as "Satellite Communications Systems" published by Wiley.

ABSTRACT

GPS signal processing in geostationary environment is more difficult than for a classical receiver on Earth in normal conditions. There are numerous differences between the GPS signals that an Earth user receives and the signals that a geostationary satellite receives. The specific and main characteristics of the GPS signal received by a geostationary satellite are the following: high C/No values only for ray tangential to the earth, very important Doppler values (+/-15kHz), and poor Dilution Of Precision factor (usually higher than 5). A GPS/Galileo receiver onboard a geostationary satellite has to deal with these specific constraints.

Several acquisition strategies can be envisaged so as to produce a point position. To reduce the delay and Doppler uncertainty and to get the navigation data, we could for example choose a strategy where some of the data (such as ephemeris or almanacs) are downloaded from Earth, but this increases the complexity and the cost of the receiver and of its integration in the satellite. Our aim in this paper is to use acquisition techniques which work in a global autonomous acquisition strategy. So the receiver does not use "aiding data". In this case, the chosen acquisition technique must be really effective at least down to the demodulation threshold, and that threshold needs to be lowered to its minimum.

The aim of this paper is to present 3 different unaided acquisition schemes and to compare their performances to process the GPS/Galileo signals in the particular context of a geostationary orbit.

The first method consists in a classical FFT acquisition. This technique will be used as a reference to evaluate the performances of the other techniques.

The second scheme called Half Bit Method (developed by M.Psiaki) is a method which allows long coherent integration time without knowing the data bit transition time. It avoids losses due to a bit transition occurring within the coherent integration time.

The last acquisition technique studied is known as "double block zero padding" method. The main interest of this method is its rapidity and also, its low computational cost.

The paper presents the test acquisition results over one standard day for a given geostationary orbit position. The work presented shows the statistics of successful acquisition as well as misdetection over one day for the three acquisition techniques.

The length of signal required to achieve a minimum successful detection rate is also investigated. Due to the weakness of the considered signals and the power difference between the different received signals inducing cross-correlation, it is often necessary to process more than 1 second sometimes around 2 or 3 seconds.

In this paper, we focus on an autonomous acquisition strategy, so we consider the receiver does not use "aiding data" downloaded from an earth link. Then, so as to perform a precise positioning, we need to demodulate the navigation message to extract the previous data. This is also necessary in order to reduce the Doppler uncertainty and so, to reduce the processing time. Thus, the paper considers several data demodulation thresholds (from 24dBHz to the usual 27dBHz value) and assesses the impact on the data demodulation and the consequence of a possible bit error on the final calculated position.

Finally, we can compare the 3 acquisition methods in regards with their efficiency towards the different values when they are processed onboard a GEO satellite.

INTRODUCTION

There is a growing interest in achieving geostationary satellites localization by using GNSS signals. However, we recall the GPS signal received in a geostationary orbit is somewhat different from the signal that a classic earth user can encounter. The specific and main characteristics of the signal received by a geostationary satellite are the following: the C/No values are spread around 15dBHz-20dBHz and roughly go up to 45dBHz; the Doppler values are very important (+/-15kHz), and the Dilution Of Precision factors are usually higher than 5.

A GNSS receiver onboard a geostationary satellite will have to deal with these specific constraints. Several acquisition strategies can be used to cope with these constraints and to produce an accurate position. Our aim in this work is to use acquisition techniques which work in a global autonomous acquisition strategy. So the receiver does not use any "aiding data", such as GPS ephemeris or almanacs uploaded from the earth. Then, the complexity, the cost and the adaptability of the receiver is lowered. With these operating constraints, our aim in this paper is to compare the performance of three different acquisition techniques.

The first part of this paper recalls the characteristics of GPS signal when processing it on a geostationary orbit. The problems we face in the geostationary orbit to develop an autonomous signal processing are also presented, notably the validity period of the ephemeris for each satellite. Indeed, to get the ephemeris of a GPS satellite, we must be able to demodulate its ephemeris at least once every four hours. Due to the C/No level and variation rate we face in the geostationary orbit, the task can be hard. Then, in a second part, we study several data demodulation thresholds so as to improve the number of satellites we can use with valid ephemeris data. If it uses a lower data demodulation threshold, the receiver is able to demodulate for longer period and more often because it can process signals with a lower C/No, and thus it extends the time the receiver can process these signals.

After determining the Space Vehicule the GEO receiver can use to compute a point position, the third part of this paper presents the three acquisition techniques we want to compare in the geostationary environment: the first one is the classic FFT acquisition method, the second one is called the Half Bit method and the last one is called the Double Block Zero Padding method. The last part of the study presents the results for the three acquisition methods over an entire day. In particular, the position error along the day is estimated by using a classic least square estimation.

GPS SIGNAL CHARACTERISTICS FOR A GEOSTATIONARY ORBIT RECEIVER

As denoted in several previous studies (**[1],[2],[3]**), the conditions for GPS signal processing are not optimal for a GEO receiver. As depicted in figure 1, the GEO orbit is around 42164km from the center of the earth. So GEO satellites are higher above the Earth than the GPS constellation orbit. Then, for most of the time, the GPS antenna does not point in the direction of the GEO satellite antenna.

Besides, as in **[1],** the delay introduced by the crossing of the ionosphere for a signal tangent to the earth can fluctuate a lot and the delay can be as important as more than 100m. To protect ourselves from such a bias, we consider an earth masking for the following of the study, i.e we assume that the masking radius of the earth is the normal radius plus 1000km which stands for the ionosphere layer. The signals coming from that direction are not considered.

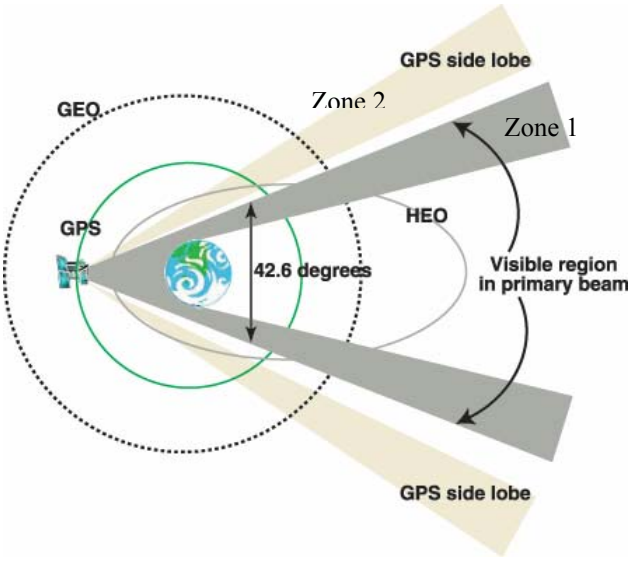

Figure 1:Geostationary satellite visibility

Let us denote zone 1the area covered by the main lobe of the GPS antenna and zone 2 the area covered by the side lobe of the GPS antenna. Due to the directivity of the GPS antenna and the GEO receiver antenna, the received signal strength quickly decreases if the GPS signal is not emitted through the main lobe of the GPS antenna. Thus, the signals have a better strength when they are emitted by satellites in zone1, at the opposite of the GEO satellite toward the earth. At each epoch, the number of GPS satellites located in this area is not large. So, in order to increase the number of visible satellite and their visibility duration, we also consider signals emitted through side lobes of the GPS antenna. Thus, we consider the satellites emitting from zone2. The received signal strength becomes far lower in this case while the elevation of the GPS satellite decreases. With the assumptions made in **[1]** (notably the GEO antenna gain pattern), we can compute the C/No of the received signals depending on the elevation of the GPS satellite toward the GEO as illustrated in figure 2.

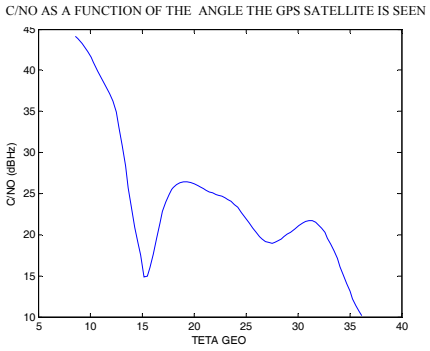

Figure 2: Global C/No from the receiver point of view with GPS (L1) satellites

Teta GEO is the off-boresight angle of the GEO antenna. The figure 2 shows that the C/No ranges from 45 dBHz to less than 15 dBHz when considering the side lobes signals. The signal strength really is weaker than for an Earth user in normal conditions. We can see that most of the received signals have strength between 20 and 25 dBHz. So, to benefit from extra measurements, the acquisition techniques will have to work at least down to these values. In compensation to these low signal levels, the visibility duration of the GPS satellites is well improved. Indeed, in the case where we only consider the GPS satellite main lobe, the GEO satellite can only 'see' 1 or 2 satellites for 58% of the time, 3 satellites for 9% of the time and no satellite for the rest of the time. The minimum of four satellites required to compute a point position measurement is not reached. The figure 3 depicts the number of satellites the GEO satellite can see with a C/No higher than 20 dBHz and 25 dBHz.

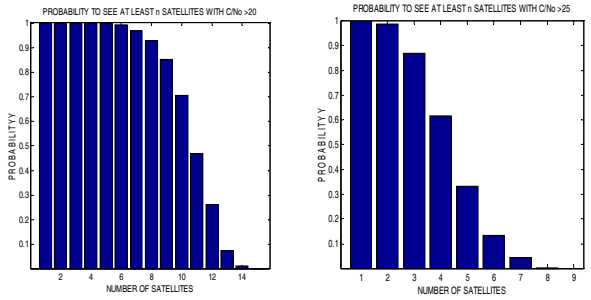

Figure 3:Probability to see at least N satellites with C/No>20 dBHz (left) and C/No>25dBHz (right)

By processing signals down to 20 dBHz, 5 satellites are always visible and more than 10 are visible for more than 50% of the time. So, the receiver should be able to compute a point position. We note that the number of visible satellites significantly decreases when we want signals with a C/No higher than 25dBHz. It is only possible to see 2 satellites at almost any time.

Another important characteristic of the signals received in the geostationary environment is their Doppler frequency values. Indeed, the velocity of the GEO is around 4km/s and then, the rate of change of the distance between the GEO satellite and the GPS satellite can vary very fast in some configurations, faster than for an earth user. So, the Doppler frequency for a GEO satellite ranges from +/- 15kHZ, which is 3 times higher than for an earth user. However, only the uncertainty on the Doppler frequency has a direct impact on the acquisition computation complexity. The number of Doppler bins to explore during the acquisition process depends on the Doppler uncertainty which is the deviation between the true Doppler and the predicted doppler. With such a Doppler uncertainty, the calculation would be too expensive in terms of time and energy consumption. So, we need to reduce the Doppler uncertainty. We remind that we want an autonomous receiver without any uplink from the Earth. One interesting solution to reduce the Doppler uncertainty is to know the almanacs or even better all the ephemeris data of the visible satellites. So, we consider that at least valid almanacs (not older than 1 week) are stored in the memory of the receiver. If it is the first ever start of the receiver, we consider that almanacs have been loaded before the geostationary satellite launching. If the receiver has already worked in live conditions, we consider the almanacs data have been demodulated during this last processing. Knowing the almanacs data and so an approximate position of the GPS satellites, the remaining Doppler uncertainty only depends on the uncertainty on the GEO receiver position and velocity, the uncertainty on the GPS time and the local oscillator drift (we assume a 1 p.p.m oscillator bias). The Doppler uncertainty falls down to only +/-2000Hz with these assumptions, and it can be even lowered by a reduction of the local oscillator drift.

Moreover, to be autonomous, the receiver must know enough valid ephemeris from visible satellite to compute its position thanks to the pseudorange measurements as we will see in the last section.

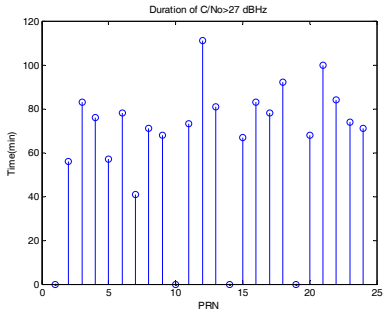

Figure 4:Duration of the C/No>27dBHz for the 24 GPS satellites over one day

The usual data demodulation threshold is set to 27dBHz for L1 C/A. The duration for each GPS satellite where their C/No is above this value is not long as shown in figure 4, where the total observation time is one day (1440 minutes).

We expect to have long periods without the possibility to demodulate the data, and as a consequence, the ephemeris data exceed their 4hours validity period. So, we cannot use those satellites to compute the GEO position. Thus, we would like to ease the demodulation of the data. In the next section we study the impact of a modification of the data demodulation threshold.

REDUCTION OF THE DATA DEMODULATION THRESHOLD

If we decrease the demodulation threshold, the period the receiver is able to demodulate the data will increase. As a consequence, the periods between two ephemeris demodulations will be shortened and we can expect we come close to a continuous availability of the ephemeris along a day, or at least, we should be able to get four or more GPS satellites with valid ephemeris to compute a point position at each epoch of the day.

The data demodulation threshold depends on the probability of bit error we accept during the processing of the data (see figure 5). As in figure 4, the period where the C/No is under the demodulation threshold are important, by taking this threshold to 27dBHz. We can consider that we could choose a lower threshold. As a consequence, the BER will increase but we have to study until what BER value we can go without degrading the demodulation too much.

The relationship between the BER and the C/No is given by the figure 5. The curve concerning the GPS L1 signal (uncoded BPSK modulation) is the right one. The relationship used in figure5 is: $\frac{C}{No} = SNR \times \frac{1}{Tp} = \frac{Eb}{No} \times \frac{1}{Tp}$

and $10\log(\frac{1}{Tp}) = 17$ with Tp=20ms.

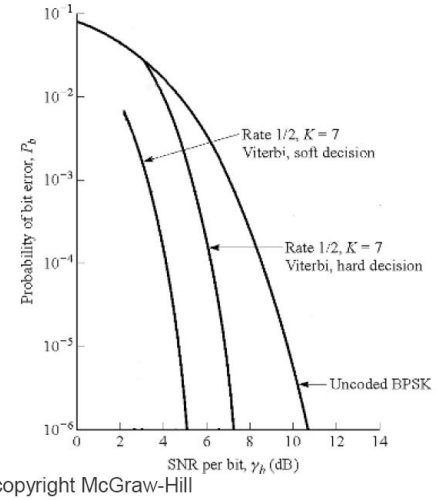

Figure 4:BER for L5 convolutional codes using soft and hard viterbi decoding and BER for uncoded BPSK transmission

As the slope of curve for the uncoded BPSK is not steep, a little decrease in the threshold implies a larger increase in the BER. We see on figure 5 that with the L5 convolutional code, the configuration is more interesting. So we have to discuss the possible and acceptable value for the BER and then, study the availability of the GPS satellites for the corresponding C/No threshold.
There are 300 bits in each of the subframe 2 and 3 where the ephemeris data are encoded. So, the message contains 600 bits where we do not want any error to occur in order to get the right ephemeris parameters. We also need to demodulate the clock correction data which are encoded by 62 bits in the subframe 1. We do not want to do more than 1 error on these 662 bits. So, we choose to study the C/No corresponding to a BER until 10e-3. The corresponding C/No is 24dBHz.
The correspondences between the C/No and the BER are the following (see figure5):

Minimum C/No for the Data demodulation threshold	Corrresponding BER	Probability to demodulate the entire ephemeris with no error $(1\text{-BER})^{662}$
26dBHz	5.10^{-5}	0.967
25dBHz	2.10^{-4}	0.88
24dBHz	10^{-3}	0.52

Figure 5: Different data demdulation threshold and the corresponding BER

The risk that an error occurs during the demodulation of the ephemeris data with the threshold put to 24 dBHz is high. The probability that an error occurs is 0.48.

The usual ephemeris validity period is 4 hours. The ephemeris data are valid from 2 hours before TOE to 2 hours after TOE, where TOE is the Time Of Ephemeris. TOE is a value broadcast in the navigation message. The ephemeris are broadcast from around 2 hours before the TOE. The same ephemeris is then broadcast to the TOE time. After this switching time, a new set of ephemeris parameter are broadcast for two hours.

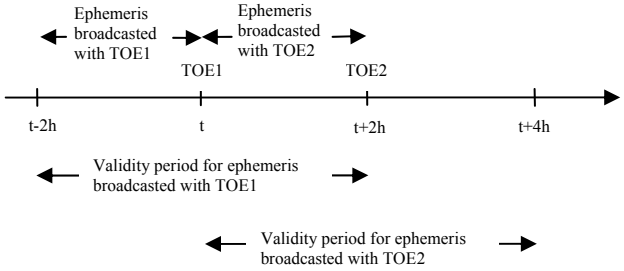

Figure 7:Ephemeris validity and ephemeris switching time

According to that ephemeris renewal scheme, we compute the number of satellites which are visible and for which the receiver has valid ephemeris data at the same time. We choose to consider that the lower bound of the C/No where the receiver is able to make pseudorange measurements with is 20 dBHz. This is convenient as we see in figure 2 and 3 that most of the signals have strength between 20 and 25 dBHz.

Data Demodulation Threshold: 26dBHz

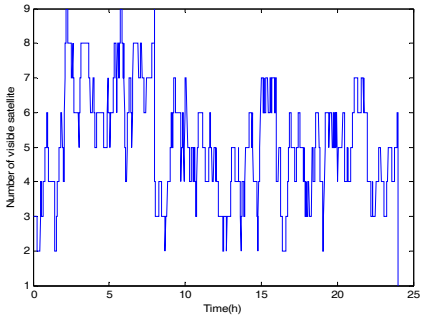

Data Demodulation Threshold:25dBHz

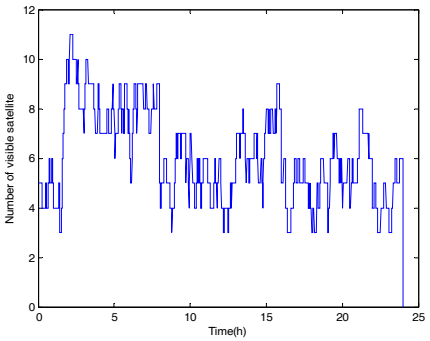

Data Demodulation Threshold: 24dBHz

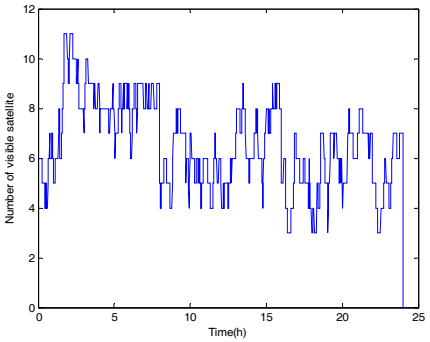

Figure 8:Number of visible PRN with valid ephemeris and C/No>20 for different data demodulation threshold

In figure 8, the first two hours are considered as an intermediate state because we have no availability indication of the GPS satellites for the 2 hours before 0h where we could have downloaded an ephemeris. The figures show that the number of useable PRN increases when the data demodulation threshold decreases. More precisely, with the 26 dBHz Data Demodulation Threshold (DDT), we face many periods during the day where the GEO receiver can only use 2 or 3 satellites. So, during these periods, the receiver cannot produce a position estimate. These periods are shortened with the 24 and 25 dBHz DDT and there are only short periods with 3

satellites. However, we consider that the probability to demodulate the entire 600 bits ephemeris data with no error is too weak with DDT=24dBHz. So for the following of the study, the DDT is taken to 25 dBHz. This is a good trade off between the number of satellites we can use to compute a position with valid ephemeris and the probability to demodulate the entire ephemeris data with no error. If we had chosen to consider that the lower bound of the C/No the receiver is able to work with is reduced to 16 dBHz, the number of useable satellites would not really improve.
With these results, we can compute the corresponding Dilution Of Precision factors.

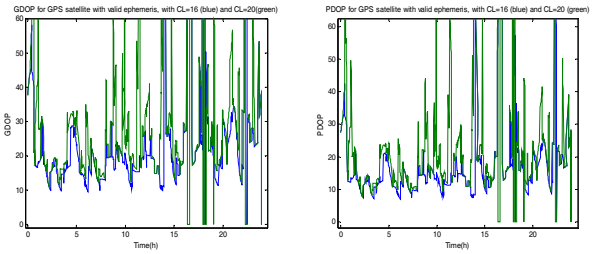

Figure 9:GDOP (left) and PDOP (right) for GPS satellites with valid ephemeris; DDT=25dBHZ

We compute the DOP for a receiver which works at 16 dBHz and 20 dBHz as depicted in figure 9. In both cases, the values are really high and the position computation will be significantly affected by these poor DOP values. The mean value of the PDOP is 18.2 and the GDOP mean value is 23 for lower acquisition bound equal to 20 dBHz (green curve in figure9). The peaks above 40 correspond to the epochs where there are only 3 or 4 satellites useable. We note that there is not really improvement with a 16 dBHz threshold working (blue curve on figure 9), so we keep this threshold to 20dBHz.

In conclusion, the acquisition method which must be implemented in the GEO receiver has to work at least down to 20 dBHz with the Data Demodulation Threshold equals to 25 dBHz.

ACQUISITION ALGORITHM

In this section, we present the three acquisition methods used to compute the GEO satellite receiver position.

1+1ms FFT acquisition method

This method is used as a reference to compare the performances of the two other.
The structure of the acquisition loop is presented in figure10. We assume that the signal has already been filtered by the RF front end filter and down-converted to the intermediate frequency f_I .

The signal has the following expression when it enters the acquisition loop:

$$s_f(kT_e) = Ad(kT_e - \tau)c_f(kT_e - \tau)\cos(2\pi f_I kT_e - \theta(kT_e)) + n(kT_e)$$

with

- d : data transmitted trough the received GPS signal.
- c_f : the filtered received spreading code.
- τ : group propagation delay.
- θ : received phase shift.
- n : white Gaussian thermal noise with PSD $N_0/2$ dB W Hz^{-1}.

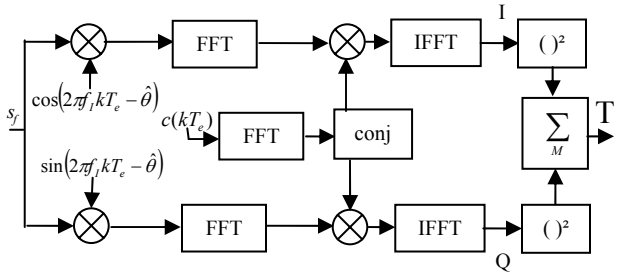

Figure 10:Acquisition loop structure

Assuming the Doppler effect, so that the phase is time dependent, the in-phase correlator output is :

$$I(n) = \frac{A}{2} \cdot d(n) \cdot \left(\frac{\sin(\pi \Delta f T_p)}{\pi \Delta f T_p} \right) \cdot R_{c_f c}(\tau(n) - \hat{\tau}(n)) \cdot \cos(\theta(n) - \hat{\theta}(n)) + n_I(n)$$

with

- n_I : centred Gaussian correlator output noise with power $\sigma_{n_I}^2 = \frac{N_0}{4T_p}$
- $R_{c_f c}$: cross-correlation between the received filtered spreading code (which has been filtered by the RF front-end filter) and the local replica code.
- $\hat{\tau}$: estimation of the group propagation delay.
- $\hat{\theta}$: estimation of the received phase shift.
- Δf : Doppler residual. $\Delta f = f_d - \hat{f}_d$.
- T_p : coherent integration time.

The principle of the acquisition depicted in figure 10 is as follows: once Tp seconds of the signal have been correlated in the FFT correlator, it is squared, and then the magnitude is stored into memory. Another Tp seconds of signal enters the loop and is processed as previously described. The magnitude is added to the previous result. This process is repeated M times, M being the non-coherent integration parameter. The whole process is repeated for each Doppler bin. The results of the

processing is the classic acqusition matrix, whose values are compared to a threshold to find the right [delay – Doppler] value which maximizes the acquisition matrix.

The minimum Tp value is 1ms. The process used in our algorithm differs a bit from the one described in figure 10. With Tp=1ms, the FFT correlation is made on 2ms of signal with 2ms of local code as shown in figure11:

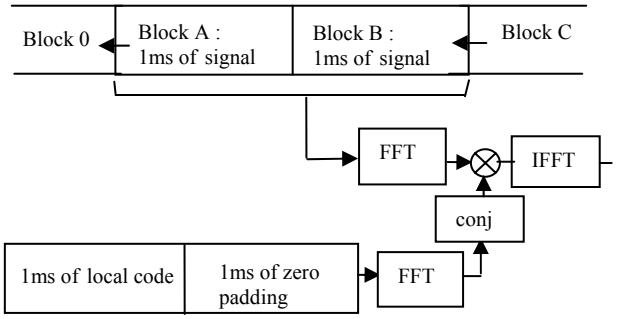

Figure 11: 1+1ms FFT correlation process

The incoming signal samples are put into a 2 ms data buffer, half of which will be replaced in a first-in first-out manner every 1 ms. The FFT of the incoming signal samples over 2 ms is taken. The extended local code replica is formed by appending 1 ms of zeros after the 1 ms of local code. The complex conjugate of the FFT of the extended replica is then computed.
The next correlation process will be carried out with block B and block C which is the millisecond coming after the block B.
This technique avoids the correlation losses that can happen if a bit transition data occurs inside the block A. Thanks to the 1ms zero padding, the FFT correlation over 2ms is not affected by the data bit transition. The switch in the sign of the samples within block A after the bit transition and block B is compensated by the way the FFT correlation works.
For coherent integration over longer periods such as Tp=5ms, Tp=10ms or Tp=Nms, we do not compute the FFT over 10ms of signal. To begin, a correlation is carried out over the first 1ms following the figure 11 process. The output is stored in memory, and then the next 1ms of signal is correlated. The process is done till the N ms and then, the N outputs stored in memory are summed before being squared. Thereafter, the next Tp ms are processed. This method increases the computational speed. As the signal strength we deal with is weak, the number of coherent and noncoherent integrations will be large and the reduction of the computational time is very important.

Half Bit acquisition method

The second acquisition method we investigate is the half bit method which is developed in **[4].**

The basic idea is to get rid of the losses due to a data bit transition occurring during a coherent summation of the signal by performing summation over time intervals which are not affected by a data bit transition.
As in the first method, the signal has the following expression when it enters the acquisition loop:

$$s_f(kT_e) = Ad(kT_e - \tau)c_f(kT_e - \tau)\cos(2\pi f_I kT_e - \theta(kT_e)) + n(kT_e)$$

Let N be the number of samples within one PRN code.
To compute the correlation of the J[th] PRN code period, let us note

$$I_{1J} = \sum_{k=JN}^{N(J+1)-1} S_f(kTe)\cos(2\pi f_I kTe)$$

$$Q_{1J} = \sum_{k=JN}^{N(J+1)-1} S_f(kTe)\sin(2\pi f_I kTe)$$

and $C_J = C(kTe)$ with $k \in [JN, N(J+1)-1]$

The correlation over the J[th] PRN code period is:

$$I_{2j} = IFFT(FFT(I_{1J}).conj(FFT(C_j)))$$

$$Q_{2J} = IFFT(FFT(Q_{1J}).conj(FFT(C_j)))$$

The summation over L PRN code period from the J_m^{th} PRN code period is:

$$I_{3J_m} = \sum_{J=J_m}^{J_m+L}(I_{2J}) \quad and \quad Q_{3J_m} = \sum_{J=J_m}^{J_m+L}(Q_{2J})$$

The non-coherent summation over M coherent summations is:

$$T = \sum_{m=0}^{M-1}(I_{3J_m})^2 + (Q_{3J_m})^2$$

Each short summation interval spans *L* PRN code periods, and they start at the PRN code periods $J_0, J_1, J_2, ...J_{M-1}$
The idea of this method is to limit *L* to 10 and to try two different intervals. The second interval is delayed by 10 milliseconds from the first.

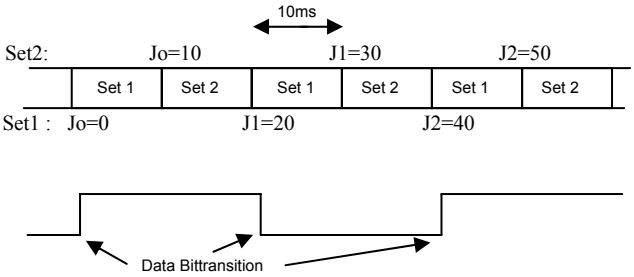

Figure 12:Construction of the 2 sets

With this temporal cut out, we are sure that at least one of the two intervals does not contain a data bit transition because transitions are separated by multiples of 20 milliseconds, the duration of a data bit. Thus, one of the two sets does not undergo losses due to the data bit transition. In figure 12, the set 2 is without any data bit transition. Moreover, the receiver does not need any

knowledge about the data bit transition time. As long as the synchro bit is not carried out, the acquisition process could face important losses due to coherent integration over a data bit transition time. Thanks to this method, one of the set is guaranteed to have no bit transitions in any of its presquaring summation intervals.
Figure 13 and figure 14 show the matrix acquisition obtained with the set 1 and the set 2. Here the data bit transition occurs in the middle of the set 1. The true code delay is 756 chips and the true Doppler is -474 Hz. The peak is not detected with the set 1 whereas the peak detected with the acquisition matrix is the right one with the set 2.

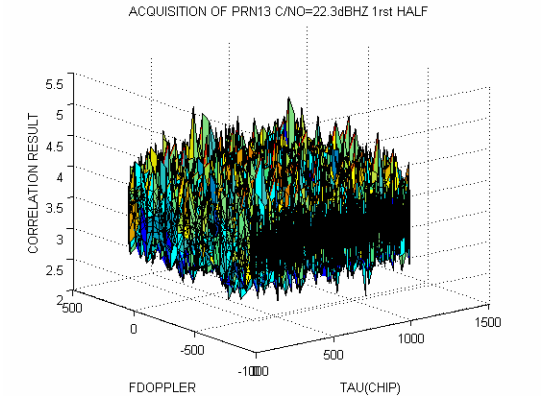

Figure 13: Acquisition matrix for the PRN13 set 1

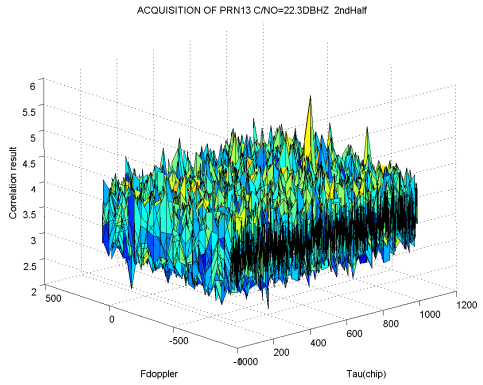

Figure 14: Acquisition matrix for the PRN13 set 2

Obviously, since this method processes an acquisition scheme over two sets of signals, the computational cost is more important than for the first method. The calculation is almost done over twice more signal length than with the first method.

Double Block Zero Padding Method

Whereas the first two acquisition methods described in this section compute the classic acquisition matrix in order to find the right delay and the right Doppler frequency which affect the signal, in this method, the delay-doppler research is not achieved following that kind of time-frequency research with the double block zero padding algorithm. The algorithm does not deal with coherent acquisition nor non coherent acquisition. The method is described in **[5]** and **[6].**
The approach to achieve signal acquisition here is to split N milliseconds of data sample into M blocks. Then, partial correlations on the M block are made to find the delay and the Doppler. The correlation principle between the different blocks is explained by the following figure:

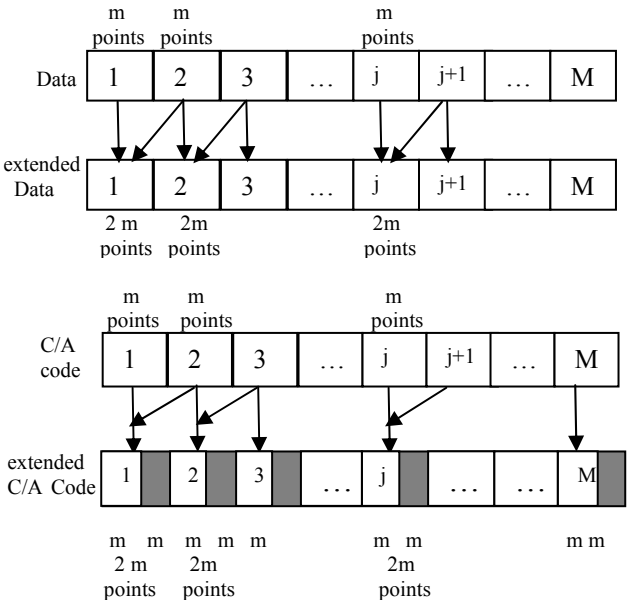

Figure 15:Construction of the extended data blocks and C/A code blocks

The grey blocks are blocks of zeros. For both the C/A code and the data, we create extended blocks of 2m points made of two blocks of m points. The C/A extended code is obtained by combining a m-points block of code and a m-points blocks of zeros. Then, each 2m-points blocks of the extended data and the corresponding extended code are FFT-correlated as shown on figure 16.

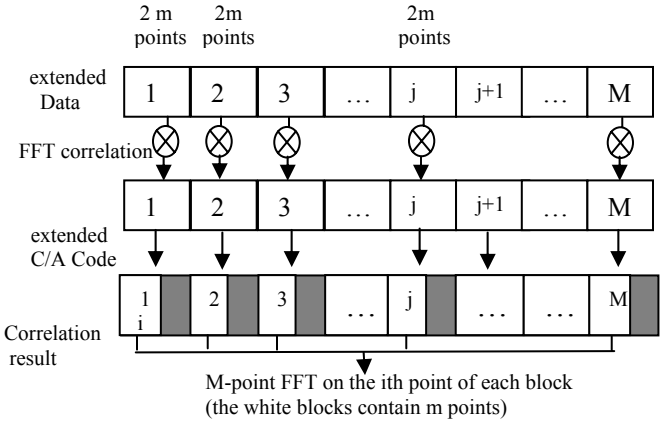

Figure 16: FFT Block correlation and FFT transformation

We only interest in the first m-points of the correlation result of each block correlation (blocks in grey in figure16). The blocks we now work with are M blocks of m-points.

The search of the delay and Doppler is done as follow: we apply an FFT to the first point of each M blocks as shown on figure 16. It results in M point vector. This process is repeated for the second point of each block, the third,… till the m^{th} point.
Then, the correlation process start again but another order of the C/A code is used. The C/A code blocks are circular permutated: the M^{th} block becomes the first, the first block becomes the second…The new C/A code block is extended as before the correlation process. We can make M permutations like this. Finally, we obtain $M \times m$ vectors of M points. The delay and Doppler are found by searching the maximum over these $M \times m$ vectors.
To give an idea of the number of subdivision we must make, an example is the easiest thing to understand: The size of the sub-division is based on the total Doppler coverage. Let's assume our Doppler coverage is ±15 kHz and the integration time is 10 ms. Therefore, the Doppler resolution is 100Hz, the total Doppler bins are M=300, and the total number of sub-division is also M=300. For M=300 and N=600,000 being the number of samples within the 10 ms, the size of the sub-division is N/M=K=2000 points. The corresponding locally generated N-points of sampled C/A-code (10x1023 chips) is also divided into M-blocks. M blocks of the C/A-code are block-by-block correlated with M blocks of data.

The performances of the three acquisition methods described in this section are evaluated in the next section for a geostationary orbit, notably the position error is computed thanks to a least square algorithm.

GEOSTATIONARY ACQUISITION RESULTS

The simulations are conducted over 24 hours. The GPS signals are simulated under MATLAB.
The simulated data carry the characteristics the GPS signals should have if they were processed by a real receiver on a geostationary orbit. For each epoch, the elevations of the GPS satellites as well as their distances with the GEO satellite are used to compute the C/No of the signals reaching the receiver. The Doppler and the transmission delay are also obtained by simulating the GEO orbit and the GPS satellites orbits.
We set the lowest acceptable signal strength to process the GPS signals. This threshold is taken at 20 dBHz. With a predicted C/No under that threshold, we will not try to acquire the corresponding satellite. As we had seen in the second section, this threshold is convenient with our requirements in term of number of useable satellites.

The Probability of false alarm is set to 10^{-5} for the three acquisition techniques
The acquisition of all visible PRN with valid ephemeris and with a C/No>20 dBHz is performed every 10 minutes during the 24 hours of simulation. At each epoch, thanks to the delay measured by the acquisition process, we compute the estimated position of the user and we can calculate the positioning error.

To achieve the performances described after, the duration of the signal we use can be as long as 3 seconds.
Depending on the C/No the receiver should get the signal coming from a PRN, we define the number of coherent and non-coherent integration carried on during the acquisition process for the first two method. We remind that the double block zero padding method does not use coherent nor non-coherent integration.

- 1+1ms FFT acquisition method

Signal strength	Coherent acquisition (ms)	Non-Coherent acquisition	Signal Duration (s)
C/No>30	1	50	0.05
30>C/No>26.5	1	200	0.2
26.5>C/No>24	5	200	1
24>C/No>22	10	150	1.5
C/No<22	10	280	2.8

- Half Bit acquisition method

Signal strength	Coherent acquisition (ms)	Non-Coherent acquisition	Total Signal Duration (s)/ Signal set duration
C/No>30	10	5	0.05/0.025
30>C/No>26.5	10	50	0.5/0.25
26.5>C/No>24	10	150	1.5/0.75
24>C/No>22	10	300	2.5/1.5
C/No<22	10	350	3.5/1.75

- Double Block Zero Padding Method

Signal strength	Signal Duration (ms)
C/No>30	100
30>C/No>26	500
26>C/No>22	1000
C/No<22	1500

For each epoch, the three algorithms compute the code delay for each visible satellite with valid ephemeris data. With these information, we compute the pseudo ranges measurements. We can compute them because we make the assumption that the GEO position is known with the uncertainty of less than 300km (which is the distance covered by 1ms of signal). Since the GEO satellite is on orbit and that orbit does not fluctuate fast, we consider our assumption to be realistic. The computed delays represent the estimated position within a 300km uncertainty.
The GEO position is estimated thanks to a classic Least Square method which is described in **[7]**. For the three methods, we obtain the following figures.
For the study, the location of the GEO satellite is set to:
[0 42164176 0]

1st Method

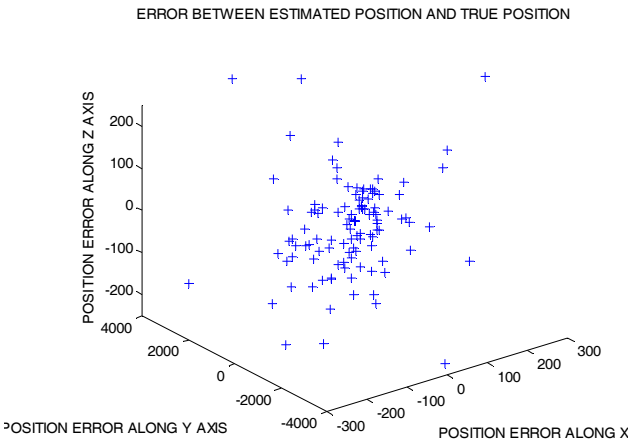

Figure17:Error between estimated position and true position

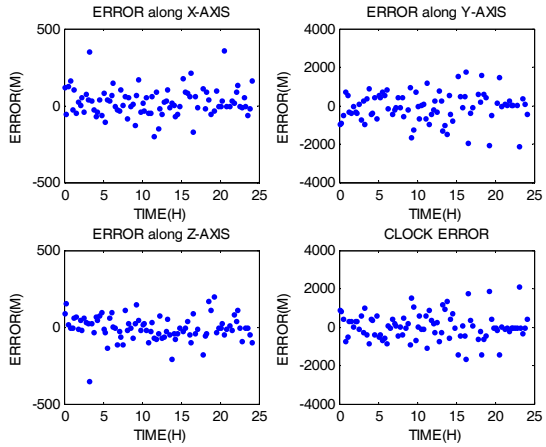

Figure18: Position and clock error calculated with every satellite with C/No>20dBHz

The computed positions remain between +/-500 meters along track and cross track as it is shown in figure 17, 18 and 19. However, the error is much more significant along the radial track (top right figure in figure 18): the error reaches more than 2500 meters in this case at some epoch. This is due to the configuration of the GPS satellites. They are all usually located in front of the GEO satellite, inside a little area, so that the accuracy of the measurements is not good along the radial track. The different GPS satellites do not provide enough informations to compute a position with a good accuracy along this axis. The receiver compute its position for 92.7% of the time when using satellites with C/No>20dBHz.

The average position error is: - 105m along track
- 588 m radial track
- 68 m cross track

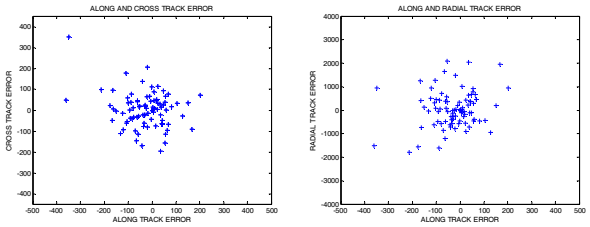

Figure19: Along and cross track error (left); along and radial track error (right)

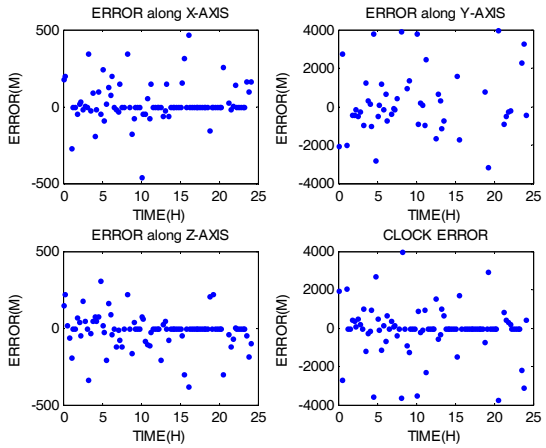

Figure 20:Position and clock error calculated with every satellite with C/No>20dBHz and valid ephemeris

The accuracy and the availability of the measurements decrease when the receiver only uses GPS satellites with valid ephemeris data. In figure 19, the dots equal to zero represent the epochs where the receiver cannot compute its position because the number of satellites which have been successfully acquired is below 4 satellites. When the receiver only uses satellites with valid ephemeris, the epochs where this phenomenon appears are numerous. Here, the receiver is able to compute its position for only 58% of the time.

2nd Method

The results are similar with the Half Bit method. The error along the radial track is bigger than the two other due to the GPS satellite configuration s for the first method. The time proportion where the receiver is able to compute its position represents 99% of the day.

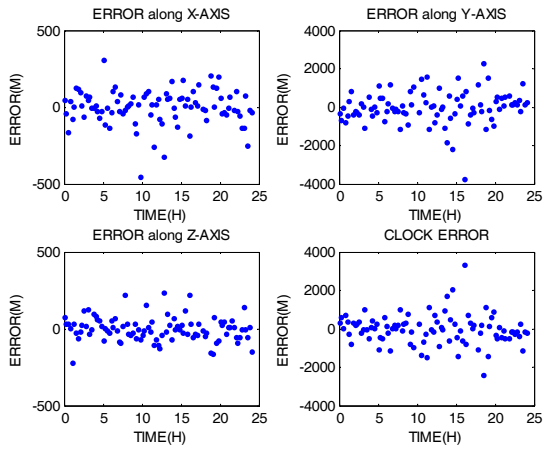

Figure21:Position and clock error calculated with every satellite with C/No>20dBHz

The mean position error is: - 105 m along track
- 767 m radial track
- 75 m cross track

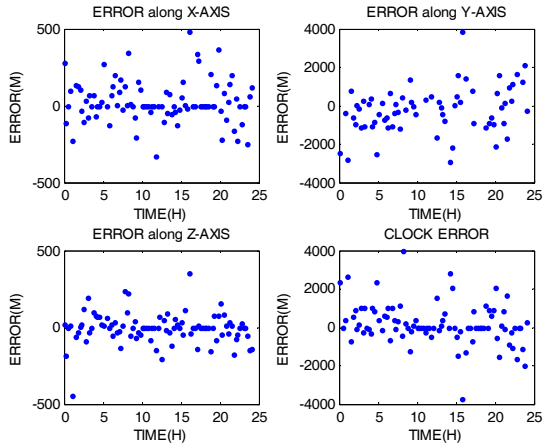

Figure22:Position and clock error calculated with every satellite with C/No>20dBHz and valid ephemeris

With this method, the use of GPS satellites with valid ephemeris data only does not affect the availability of the measurements as it does for the first method.
The duration where the receiver is able to compute its position represents 77% of the day. So it is 20% more than the first method. The second method seems more interesting in this case. Its accuracy is lower but it is more interesting to be able to compute the position more often.

3rd Method

With this method, the receiver can compute its position for 78% of the time by using all visible satellites with C/No>20dBHz and for 50% of the time by using only GPS satellites with valid ephemeris data as shown on figure 23 and 24. It is the worst performance of the three acquisitions techniques. It is only 8% less than the first acquisition method when we use satellites with valid ephemeris.

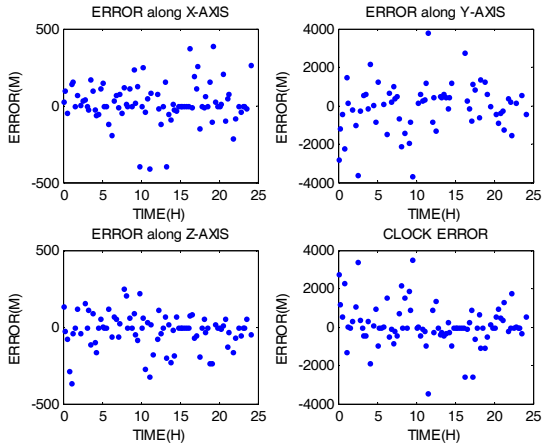

Figure23: Position and clock error calculated with every satellite with C/No>20dBHz

The average position error is: - 133 m along track
- 1008 m radial track
- 214 m cross track

This method is the less accurate among the three. However, it requires less signal to achieve the positioning.

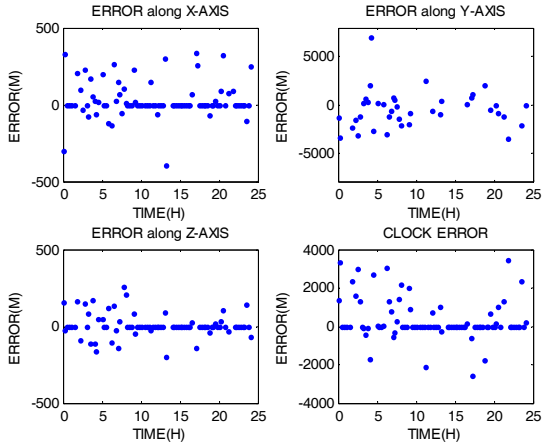

Figure 24:Position and clock error calculated with every satellite with C/No>20dBHz and valid ephemeris

The computational cost of the 3 methods has not been investigated but the first two are really time and power consuming. This last method runs more than 10 time faster than the two other method under Matlab. With the Double Block Zero Padding acquisition method the performances are less interesting because there are too many epochs where the receiver is not able to compute its position. However, for a real low cost, low consumption receiver with low requirements in terms of position computation availability, this method can be a good trade off.

The probability of misdetection is analysed prosecuted for each acquisition method. Here, the probability of

misdetection encompasses the detections missed (no signal detected) and the false detection (the acquisition process find a value above the threshold but not at the right place). Pmd have the following values for the three acquisition methods:

Probability of misdetection	Pmd with all visible satellite	Pmd with satellites with valid ephemeris
1st method	0.26	0.31
2nd method	0.26	0.30
3rd method	0.40	0.44

The Double Block Zero Padding method has a Pmd higher than the two other. In this method, weak signals are more sensitive to a strong signal than in the two other one methods. So, the number of successful acquisitions with a low C/No is very weak for this method as we see in the next table.

The performances of the three methods can be assessed by studying the percentage of successful and unsuccessful acquisitions depending on the C/No of the received signal. The following table presents the number and the percentage of successful acquisitions for several signal strength.

	C/No>30	30>C/No>26	26>C/No>24	24>C/No>22	22>C/No>20
1st method	76/94= 81%	75/100= 75%	176/279= 63%	43/67= 64%	74/103= 71%
2nd method	84/94= 89%	82/100= 82%	137/279= 49%	43/67= 64%	54/103= 52%
3rd method	76/94= 80%	53/100= 53%	198/279= 70%	32/67= 47%	38/103 36%

The second method works better than the first one. Surprisingly, the percentage of successful acquisition is low for a C/No between 24 and 26 dBHz. The minimum duration of the signal for that kind of signal strength may have been under evaluated. The unsuccessful acquisition become important when C/No is below 22 dBHz. In this case, the signal strength difference between the strongest satellite in acquisition and the weak satellites (with C/No<24dBHz) may be larger than the Gold code isolation which is 24 dB. Then, the receiver has to deal with strong crosscorrelations and so, the weak signals are not easy to acquire.

	Average number of visible sats with C/No>20dBHz	Average number of visible sats with valid ephemeris and C/No>20dBHz	Average number of successful acquisition with every sat	Average number of successful acquisition with valid ephemeris only
1st Method	10.13	6.62	7.45	4.58
2nd Method	10.13	6.62	7.71	4.91
3rd Method	10.13	6.62	5.65	4.05

This table shows the average number of satellites for the four conditions of our study.

The first line is the average number of satellite the receiver sees with a C/No>20 dBhz. The second line show the average number of satellites with both a C/No>20dBHz and valid ephemeris.

The last two lines show the average number of satellite with successful acquisition in the two previous cases.

When considering satellites with both valid ephemeris and C/No>20dBHz, the average value is less than 5 for the 3 methods. So, there are many epochs where the receiver cannot process more than 4 satellites to compute its position

CONCLUSION

Three acquisition techniques have been presented in this study and their performances have been estimated in the special case of a geostationary orbit autonomous receiver. The accuracy of the position as well as the availability of the position computation have been investigated. The first two methods present better results in terms of accuracy and availability but they have a much more significant computational cost.

We considered in this work the acquisition of GNSS signals without aiding or broadcast data. So, we tried, by lowering the data demodulation threshold, to improve the number of visible satellite with valid ephemeris along the day. Despite the reduction of the data demodulation threshold by 2 dB (25dBHz compared to the classical 27 dBHz for GPS L1) which increases the number of useable satellites with valid ephemeris, it remains many epochs where the number of useable (valid ephemeris and C/No>20dBHz) and successfully acquired satellites is not enough to compute the receiver position. This happens with all the three methods. The Half Bit method is more robust in this case, and for more than 75% of the time, the receiver is still able to compute its position.

To solve this problem for the remaining time with less than 3 satellites, the use of an orbital filter could be really interesting. Indeed, it should allow the receiver to compute its position with less than four successfully acquired satellites, because in orbit, the path of a geostationary satellite is well known.

ACKNOWLEDGMENTS

The figure1 is extracted from a GPS world article. The article entitled “Autonomous GPS Positioning at High Earth Orbit’, april2006. We thank the authors (W.Bamford, N Winternitz, C Hay). Thank you to everybody at the ENAC lab for the intensive use of their computers.

REFERENCES

[1] B.Chibout,C.Macabiau *Investigation of new processing techniques for geostationary satellite positioning* ION NTM 2006

[2] *Tracking of geostationary satellites with GPS, final presentation* ESTEC 1994

[3] J.L Ruiz, C.H Frey *Geosynchronous Satellite use of GPS* ION GNNS 2005

[4] M. Psiaki *Block Acquisition of weak GPS signals in a software receiver* ION GPS 2001

[5] D. Lin, J.B.Y Tsui *Direct P(Y)-Code Acqusition algorithm for software GPS receiver* ION GPS 99

[6] D. Lin, J.B.Y Tsui *Comparison of acquisition methods for software receiver* ION GPS 2000

[7] C.Macabiau *RAIM Performance in Presence of Multiple Range Failures* ION NTM 2005